

Institutionen för systemteknik

Department of Electrical Engineering

Examensarbete

Vehicle Mass and Road Grade Estimation using Kalman Filter

Examensarbete utfört i Fordonssystem
vid Tekniska högskolan vid Linköpings universitet
av

Erik Jonsson Holm

LiTH-ISY-EX--11/4491--SE

Linköping 2011



Linköpings universitet
TEKNISKA HÖGSKOLAN

Vehicle Mass and Road Grade Estimation using Kalman Filter

Examensarbete utfört i Fordonssystem
vid Tekniska högskolan i Linköping
av

Erik Jonsson Holm

LiTH-ISY-EX--11/4491--SE

Handledare: **Tomas Nilsson**
ISY, Linköpings universitet

Lei Feng
Volvo Technology

Examinator: **Jan Åslund**
ISY, Linköpings universitet

Linköping, 1 August, 2011

	Avdelning, Institution Division, Department Vehicular Systems Department of Electrical Engineering Linköpings universitet SE-581 83 Linköping, Sweden		Datum Date 2011-08-01
	Språk Language <input type="checkbox"/> Svenska/Swedish <input checked="" type="checkbox"/> Engelska/English <input type="checkbox"/> _____	Rapporttyp Report category <input type="checkbox"/> Licentiatavhandling <input checked="" type="checkbox"/> Examensarbete <input type="checkbox"/> C-uppsats <input type="checkbox"/> D-uppsats <input type="checkbox"/> Övrig rapport <input type="checkbox"/> _____	ISBN _____ ISRN LiTH-ISY-EX--11/4491--SE Serietitel och serienummer ISSN Title of series, numbering _____
URL för elektronisk version http://www.control.isy.liu.se http://www.ep.liu.se			
Titel Estimering av fordonsvikt och vägglutning med hjälp av Kalman filter Title Vehicle Mass and Road Grade Estimation using Kalman Filter Författare Erik Jonsson Holm Author			
Sammanfattning Abstract <p>This master thesis presents a method for on-line estimation of vehicle mass and road grade using Kalman filter. Many control strategies aiming for better fuel economy, drivability and safety in today's vehicles rely on precise vehicle operating information. In this context, vehicle mass and road grade are crucial parameters.</p> <p>The method is based on an extended Kalman filter (EKF) and a longitudinal vehicle model. The main advantage of this method is its applicability on drivelines with continuous power output during gear shifts and cost effectiveness compared to hardware solutions.</p> <p>The performance has been tested on both simulated data and on real measurement data, collected with a truck on road. Two estimators were developed; one estimates both vehicle mass and road grade and the other estimates only mass using an inclination sensor as an additional measurement. Tests of the former estimator demonstrate that a reliable mass estimate with less than 5% error is often achievable within 5 minutes of driving. Furthermore, the root mean square error of the grade estimate is often within 0.6°. Tests of the latter estimator show that this is more accurate and robust than the former estimator with a mass error often within 2%. A sensitivity analysis shows that the former estimator is fairly robust towards minor modelling errors. Also, an observability analysis shows under which circumstances simultaneous vehicle mass and road grade is possible.</p>			
Nyckelord Keywords Kalman filter, Vehicle model, Non-linear observability			

Abstract

This master thesis presents a method for on-line estimation of vehicle mass and road grade using Kalman filter. Many control strategies aiming for better fuel economy, drivability and safety in today's vehicles rely on precise vehicle operating information. In this context, vehicle mass and road grade are crucial parameters.

The method is based on an extended Kalman filter (EKF) and a longitudinal vehicle model. The main advantage of this method is its applicability on drivelines with continuous power output during gear shifts and cost effectiveness compared to hardware solutions.

The performance has been tested on both simulated data and on real measurement data, collected with a truck on road. Two estimators were developed; one estimates both vehicle mass and road grade and the other estimates only mass using an inclination sensor as an additional measurement. Tests of the former estimator demonstrate that a reliable mass estimate with less than 5% error is often achievable within 5 minutes of driving. Furthermore, the root mean square error of the grade estimate is often within 0.6° . Tests of the latter estimator show that this is more accurate and robust than the former estimator with a mass error often within 2 %. A sensitivity analysis shows that the former estimator is fairly robust towards minor modelling errors. Also, an observability analysis shows under which circumstances simultaneous vehicle mass and road grade is possible.

Acknowledgments

This master thesis was carried out at Volvo Technology, the innovation centre within the Volvo Group. It has been very interesting to get the opportunity to do my thesis in this environment. First and foremost, I would like to express my sincere gratitude to my supervisor at Volvo Technology Lei Feng for all feedback on my work, great support and interesting discussions. Also, I would like to thank my supervisor at Linköping university Tomas Nilsson for good guidance and good answers on my questions. Generally, I would like to thank the people I have been in contact with at Volvo and the university for good answers on my questions.

Contents

1	Introduction	1
1.1	Related Work	2
1.2	Outline	2
2	Project Prerequisites	5
2.1	Data Collection	5
2.2	Sensors	5
3	System Model	9
3.1	Vehicle model	9
3.1.1	Driveline	10
3.1.2	External Forces	12
3.1.3	Combining the equations	13
3.2	State Space Model	14
3.2.1	Process Equation	15
3.2.2	Measurement Equation	16
3.3	Model Validation	16
4	State Estimation	19
4.1	Observability Analysis	19
4.2	Kalman filter	21
4.3	Estimator Implementation	24
5	Results	27
5.1	Testing with Simulated Data	27
5.1.1	Mass and Grade Estimation	27
5.2	Testing with Real Measurement Data	29
5.2.1	Mass and Grade Estimation	29
5.2.2	Mass Estimation	30
5.3	Sensitivity Analysis	31
6	Conclusions and Future Work	35
6.1	Conclusions	35
6.2	Future Work	35

Bibliography

37

Chapter 1

Introduction

Fuel economy, drivability and safety are prioritized areas for today's automotive manufacturers. More and more advanced embedded control systems are utilized to improve these areas. The performance of these control systems can be improved if precise vehicle operating information is used. To obtain this information the vehicle force balance equation needs to be solved in real time. In this equation, vehicle mass and road grade are crucial parameters. For example, transmission management systems often use automatic gear selection in order to determine the most appropriate gear at the moment. The functionality of this control strategy relies on an accurate prediction of the required driving torque. The determination of the driving torque in turn relies on accurate values of the vehicle mass and road grade. Incorrect values of these parameters could lead to an inappropriate gear selection that increases fuel consumption and reduces drivability.

Vehicle mass and road grade need to be determined on-board since both are changing parameters. The mass of a truck can for example increase by some 400 % after loaded. Currently, vehicle mass is determined in different ways depending on the vehicle configuration. Trucks equipped with pneumatic suspension and electronically controlled suspension, ECS, are able to measure the vehicle mass directly through the air pressure, however, this configuration is not present in all trucks. Current mass estimator utilizes the dynamics during a gear shift in order to estimate the mass. As drivelines capable of continuous power output during gear shifts evolve, this mass estimation method becomes less applicable. The reason is that it requires time of no propulsive power to function. Moreover, the present performance is not satisfying. Road grade is measured with an inclination sensor in the trucks equipped with I-Shift transmission.

Measuring vehicle mass and road grade with in-vehicle sensors add manufacturing cost. Therefore, estimating the parameters using software and microprocessor technology in combination with standard truck sensors becomes an interesting alternative.

The primary aim of this thesis is to develop an estimator that estimates vehicle mass and road grade simultaneously. Seeing the popularity of the inclination sensors in Volvo vehicles, an estimator that only estimates the vehicle mass is also

investigated.

1.1 Related Work

There are a lot of papers written within the field of vehicle mass and road grade estimation. Below is a short summary of what has been done before, including their different aims, approaches and prerequisites.

Simultaneous estimation of vehicle mass and road grade has been performed in [21], which uses recursive least squares, RLS, with multiple forgetting factors. For the initialization, least squares method is performed on a data batch to find a good initial guess. Lingman and Schmidtbauer [17] use an extended Kalman filter, EKF, and model road grade as a first order process. The authors analyse both the case of using of vehicle speed as the only measurement and the case of additionally using a longitudinal accelerometer. Kolmanovsky and Winstead [23] use an active estimator to enhance parameter identifiability through the use of an EKF for parameter estimation, and model predictive control, MPC, to control vehicle speed. Within Volvo Technology, a pre-study [7] was carried out in 2010 using EKF in order to estimate mass and grade simultaneously.

Reports on estimation of vehicle mass have been made by [5] and [8] for example. The former uses an adaptive EKF, without road grade information. The latter uses RLS and an inclination sensor signal together with vehicle speed as input. A different approach was carried out by [6] and [11]. Their analyses show that road grade only affects vehicle dynamics at low frequencies. Thus, applying a band-pass filter for extracting the high frequency components of the acceleration and force signals would eliminate road grade from the mass estimation problem. During this master thesis, their ideas were tested, but due to time limits and unpromising results this approach was not pursued. Fathy et.al [6] also review different mass estimation methods. They distinguish between averaging or event-seeking algorithms. An averaging algorithm continuously updates the estimate whereas an event-seeking one monitors specific events such as sharp acceleration or deceleration. It also classifies estimation method based on the dynamics used; suspension dynamics, lateral/yaw dynamics, powertrain dynamics and longitudinal dynamics. This thesis falls into the group of methods using longitudinal dynamics and a combination of event-seeking and averaging.

For road grade estimation, Bae et.al [4] and Sahlholm [19] use a GPS signal in combination with a vehicle model to estimate grade. The latter uses EKF and stores the estimations. These are then merged with estimates created previously when the truck passed the same road in order to create a road map. Johansson [14] and Hellgren [13] are estimating road grade through altitude information and an EKF, without using a model of vehicle dynamics.

1.2 Outline

Chapter 2 presents the prerequisites for the project, which includes the sensors used and data collection. Chapter 3 derives a state space model of the vehicle

longitudinal motion and validates the model. Chapter 4 gives an observability analysis, briefly reviews the Kalman filter and presents the design of the estimator. Chapter 5 presents the results for simulated and real measurement data and provides a sensitivity analysis. Chapter 6 gives conclusions and directions for future work.

Chapter 2

Project Prerequisites

This chapter summarizes the prerequisites for this project. The data collection and used sensors are described.

2.1 Data Collection

This section describes how the real measurement data and the simulated data was obtained.

Real Measurement Data

The vehicle used when collecting the data was a truck with a trailer connected and a weight of 33 865 kg, weighed on a scale. It was equipped with an I-Shift transmission, which is an automatic gear changing system from Volvo. Three test runs were analysed. In Figure 2.1 and 2.2 one of the test runs is presented. It contains an acceleration phase from standstill to around 30 m/s and then continued driving around that speed. The other two has principally the same features. More information about the data collection can be found in [20].

Simulated Data

The existing simulation environment within Volvo, VSim+, was used to create simulated data. VSim+ is implemented in Matlab Simulink and contains numerous alternatives to analyse different scenarios.

2.2 Sensors

The sensor signals are retrieved from the CAN-bus, which is a communication network between the different control units in the vehicle. Below follows a short explanation for each of the used sensors.

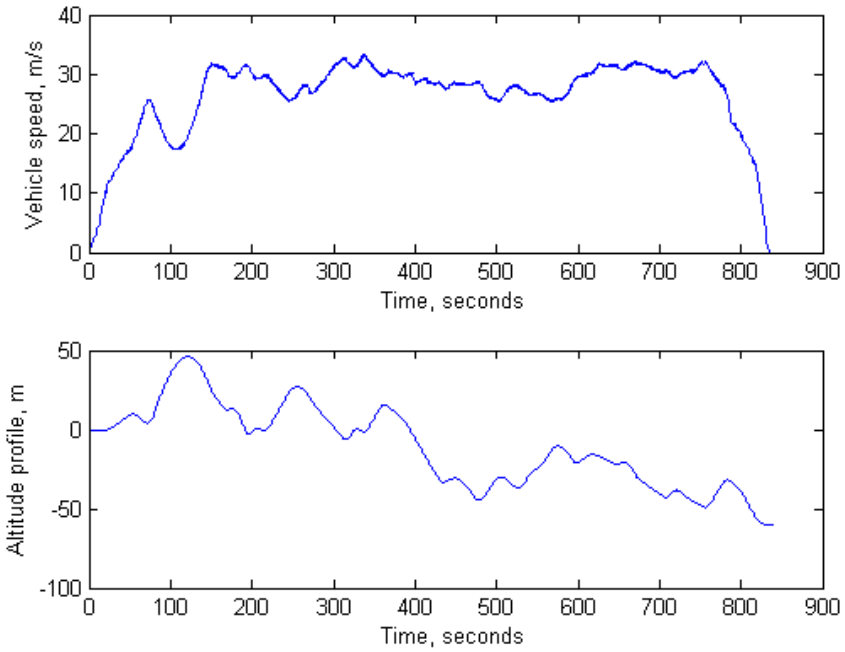


Figure 2.1. Driving route, speed and altitude profile.

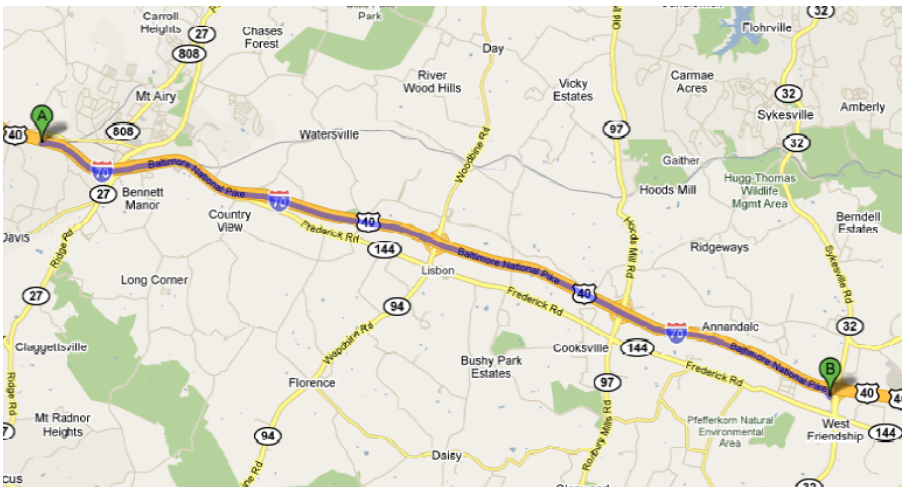


Figure 2.2. Driving route, seen from a map perspective.

Vehicle Speed

The vehicle speed is taken from the front axle wheel speed sensors, which belong to the Electronic Brake System, EBS.

Engine Torque

The engine torque is calculated by using a mathematical model, which takes the amount of injected fuel into consideration. The torque is given at a cross section of the engine output shaft. The signal is more accurate during steady-state conditions than during transients.

Gear Ratio

This is a value between 1 (12th gear) and almost 15 (1st gear) for the transmission used in this project.

Overall Gearing

Overall gearing indicates the travelled distance in the format millimeters per engine revolution.

Gear Shift In Process

The value of gear shift in process indicates when a gear shift is under process.

Brake

This brake signal indicates when the brake is applied. No information about the actual brake force was available due to difficulties to model brake force accurately.

Road Grade

Road grade measurement is based on an accelerometer on the Transmission Electronic Control Unit, TECU. The sensor, called inclination sensor, is however not present in all vehicle configurations. For more information, please refer to [16].

Sampling Interval

An analysis made during the later part of the thesis showed that a sampling interval around 170 ms would be enough. All calculations, however, was made with the original data sampling interval, 20 ms. The analysis was made by analysing the bandwidth of the speed, torque and inclination signals and choose the sampling frequency to be 10 times the bandwidth, [18]. As large sampling interval as possible is desirable in order to reduce computational burden and numerical problems.

Chapter 3

System Model

This chapter presents the longitudinal dynamics of the vehicle. The equations are gathered in a state space model, which will later be used in the estimator implementation. The chapter ends with a validation of the model and points out the conditions where the model is reliable.

3.1 Vehicle model

This section derives a complete model of the vehicle longitudinal dynamics. The basic approach is to treat the vehicle as a lumped mass. Underlying assumptions are explained throughout the text. A thorough derivation can be found in for example [9] or [15]. Fundamental for this derivation is Newton's Second Law, which is applicable to both translational and rotational systems:

Translational systems

$$\sum F = m\dot{v} \tag{3.1}$$

Rotational systems

$$\sum T = I\dot{\omega} \tag{3.2}$$

where $\sum F$ is the sum of all forces acting on a body, m is its mass and \dot{v} its translational acceleration. Furthermore, $\sum T$ is the sum of all torques acting on a body, I is its rotational moment of inertia and $\dot{\omega}$ its rotational acceleration.

A vehicle is affected by forces both externally and internally. The external forces arise from aerodynamic drag, rolling resistance and gravitational force. Internally, the driving force is originated from the combustion within the engine and transmitted through the driveline to the ground. A free body diagram of a truck in a longitudinal motion is shown in Figure 3.1. Equation (3.1) in the longitudinal direction yields:

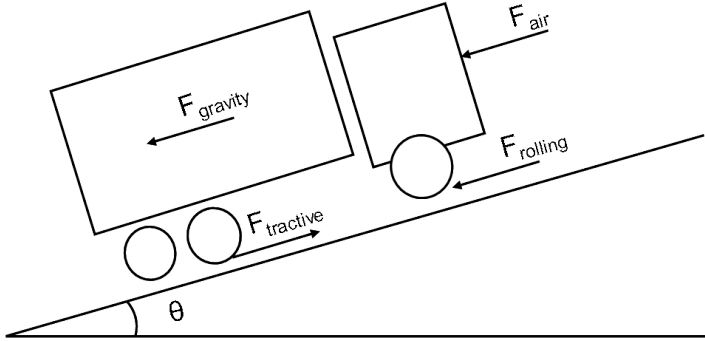


Figure 3.1. Free body diagram of a truck going uphill.

$$F_{tractive} - F_{air} - F_{roll} - F_{gravity} = m\dot{v} \quad (3.3)$$

where m is the vehicle mass and \dot{v} is the vehicle acceleration. Modelling of the forces on the left-hand side of Equation (3.3) are done in the sections below starting with a driveline model to find $F_{tractive}$ and then modelling of the external forces, F_{air} , F_{roll} and $F_{gravity}$. Finally the equations are combined into a complete driveline model.

3.1.1 Driveline

The driveline consists of an engine, clutch, transmission, propeller shaft, final drive, axle shafts and wheels, see Figure 3.2. These are all combinations of rotating parts with a rotational moment of inertia. Their dynamics are described by the Newton Second Law for rotational systems, i.e, Equation (3.2). Within a driveline, high frequency phenomena such as driveline oscillations due to torsional effects on the shafts occur. Moreover, when the torque changes abruptly, backlash effects can occur due to play between different parts of the driveline. However, the output torque at the wheels is not considered to be significantly affected by such effects most of the time. Therefore, the driveline is assumed stiff, which simplifies the derivation. Below, each component of the driveline is analysed.

Engine

- The engine is the source of the propulsive power. The output torque of the engine is denoted T_t , where subscript t indicates that it is input torque to the transmission, and described by

$$T_t = T_e - I_e\dot{\omega}_e \quad (3.4)$$

where T_e is the engine torque, the internal engine friction is here included in T_e . I_e is the engine inertia, $\dot{\omega}_e$ is the rotational acceleration of the output

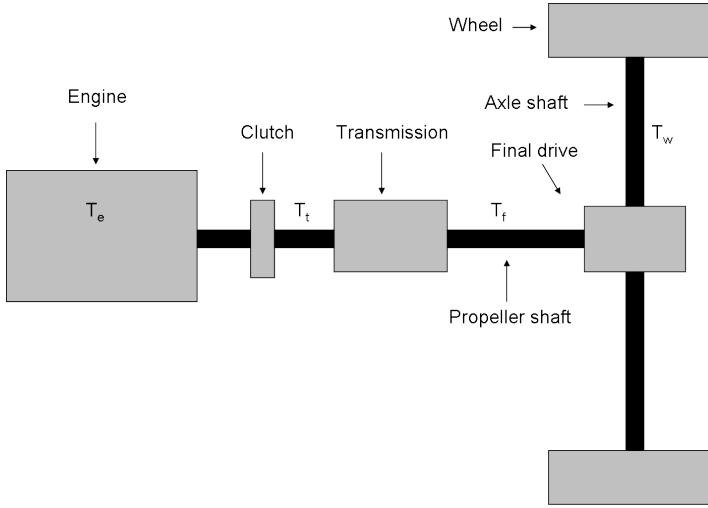


Figure 3.2. A schematic figure of a vehicle driveline. The main components of the driveline and the torques, relevant for the driveline model, are marked out in the figure.

shaft of the engine and T_t is the output torque of the engine. The inertia of the clutch is lumped with the engine inertia, therefore the clutch is not treated separately here.

Transmission

- The purpose of the transmission is to match engine speed to desired vehicle speed. The output torque is amplified by the gear ratio and decreased by inertial losses according to

$$T_f = (T_t - I_t \dot{\omega}_e) i_t \quad (3.5)$$

where I_t is the transmission inertia, as seen from the input side, i_t is the gear ratio of the transmission and T_f is the output torque from the transmission. Subscript f denotes final drive. The gear ratio, i_t , changes for each gear, but since it is piecewise constant, no time derivatives of i_t will occur.

Final drive

- The final drive turns the power flow 90° and amplifies the output torque in the same way as the transmission. However, the final drive gear ratio is fixed.

$$T_w = (T_f - I_f \dot{\omega}_p) i_f \quad (3.6)$$

where, I_f is the inertia of the final drive and the propeller shaft, lumped together. i_f is the numerical ratio of the final drive, $\dot{\omega}_p$ is the rotational acceleration of the propeller shaft and T_w is the torque acting on the wheel.

Wheel

- The torque at the axles provide a tractive force to accelerate the wheels.

$$F_{tractive}r_w = (T_w - I_w\dot{\omega}_w) \quad (3.7)$$

where I_w includes inertia from both wheels and axles shafts, $\dot{\omega}_w$ is the rotational acceleration of the wheel, r_w is the radius of the wheel and $F_{tractive}$ is the tractive force at the ground.

Since no torsional effects are considered the rotational accelerations given above are related to each other only through the gear ratios.

$$\dot{\omega}_p = i_f \dot{\omega}_w \quad (3.8)$$

$$\dot{\omega}_e = i_t \dot{\omega}_p = i_t i_f \dot{\omega}_w = i_{tf} \dot{\omega}_w \quad (3.9)$$

$$i_{tf} = i_t i_f \quad (3.10)$$

Moreover, under the assumption that there is no slip, i.e, the rolling condition is valid, the vehicle acceleration could be written as the wheel rotational acceleration times the wheel radius.

$$r_w \dot{\omega}_w = \dot{v} \quad (3.11)$$

The tractive force at the ground can now be expressed by combining the equations (3.4) to (3.11).

$$F_{tractive} = \frac{T_e i_{tf}}{r_w} - (I_e + I_t + \frac{I_d}{i_g^2} + \frac{I_w}{i_{tf}^2}) \frac{i_{tf}^2 \dot{v}}{r_w^2} \quad (3.12)$$

Mechanical losses of the driveline components have not yet been modelled. The effect of mechanical losses can be approximated by multiplying an efficiency to the first term on the right-hand side of (3.12). Also let $u_g = i_{tf}/r_w$.

$$F_{tractive} = T_e u_g \eta_{tf} - (I_e + I_t + \frac{I_d}{i_t^2} + \frac{I_w}{i_{tf}^2}) u_g^2 \dot{v} \quad (3.13)$$

Gillespie [9] points out that the tractive force (3.13) has two components. The first term on the right-hand side corresponds to the steady state tractive force, which is necessary to overcome the external forces, described in Section 3.1.2. The second term on the right-hand side models the loss of tractive force due to the inertia of the driveline.

3.1.2 External Forces

In this section, the external forces aerodynamic drag, rolling resistance and gravitational force are presented.

Aerodynamic drag

- The aerodynamic drag depends on the dynamic pressure and is thus proportional to the squared speed.

$$F_{air} = \frac{1}{2} \rho_{air} c_d A_f v^2 \quad (3.14)$$

where ρ_{air} is the air density, c_d is the aerodynamic drag coefficient and A_f is the frontal area of the vehicle.

Rolling resistance

- The rolling resistance is an effect of the deformation of the wheels. The coefficient increases with higher load and speed. A list of values of the coefficient of rolling resistance in different situations is given in [1]. Other common models than the one given in equation (3.15) include vehicle speed [9]. Such a model has been analysed but no real improvements was achieved.

$$F_{roll} = f_r m g \cos(\theta) \quad (3.15)$$

where f_r is the coefficient of rolling resistance, g is the gravitational constant and θ is the road grade. In (3.15) it would be possible to assume small angles, which would yield $\cos(\theta) = 1$. That assumption has not been done here, instead the relations (3.19) has been applied, which leads to a convenient expression.

Gravitational force

- The component of the gravity vector acting in the longitudinal direction contributes to a resistive force when climbing a hill and a driving force when going downhill.

$$F_{gravity} = m g \sin(\theta) \quad (3.16)$$

3.1.3 Combining the equations

Combining Equation (3.14) to (3.16) with (3.13) and (3.3) yields (3.17). The rotational inertias from (3.13) have been given the name m_r and lumped in with the mass.

$$(m + m_r) \dot{v} = T_e u_g \eta_{tf} - \frac{1}{2} \rho_{air} c_d A_f v^2 - m g (\sin(\theta) + \cos(\theta) f_r) \quad (3.17)$$

$$m_r = (I_e + I_t + \frac{I_d}{i_g^2} + \frac{I_w}{i_{tf}^2}) u_g^2 \quad (3.18)$$

Using the following relation makes a function of the road grade angle appearing linearly, [21].

$$\sin(\theta) + \cos(\theta) \tan(y) = \frac{\sin(\theta + y)}{\cos(y)} \quad (3.19)$$

Let $y = \arctan(f_r)$, then (3.17) and (3.19) yield:

$$(m + m_r)\dot{v} = T_e u_g \eta_{tf} - \frac{1}{2} \rho_{air} C_d A_f v^2 - m \frac{g}{\cos(\arctan(f_r))} \sin(\theta + \cos(\arctan(f_r))) \quad (3.20)$$

Define some variable substitutions to simplify the expression.

$$\beta_r = \cos(\arctan(f_r)) \quad (3.21)$$

$$\phi_1 = \frac{1}{m} \quad (3.22)$$

$$\phi_2 = \sin(\theta + \beta_r) \quad (3.23)$$

$$\alpha_1 = \frac{1}{2} \rho_{air} C_d A_f \quad (3.24)$$

$$\alpha_2 = \frac{g}{\beta_r} \quad (3.25)$$

This yields the final expression.

$$\dot{v} = \frac{\phi_1 (T_e u_g \eta_{tf} - \alpha_1 v^2) - \alpha_2 \phi_2}{1 + \phi_1 m_r} \quad (3.26)$$

which is non-linear in v and ϕ_1 .

3.2 State Space Model

A state space model was used for estimation of the vehicle mass and road grade. It consists of a deterministic part and a stochastic part. The deterministic part describes how the state estimate propagates in time. The stochastic part describes how the confidence interval changes. For further explanation, see for example [10]. The state space representation of the system is written in the following form

$$\dot{x} = f(x, u, w) \quad (3.27)$$

$$z = h(x, e) \quad (3.28)$$

where (3.27) represents the process equation and (3.28) represents the measurement equation. These are further presented below.

3.2.1 Process Equation

Augmenting Equation (3.26) with the two states ϕ_1 and ϕ_2 yields a state space model according to Equation (3.27) and a convenient way to estimate the vehicle mass and road grade through the augmented states. The dynamics of the states ϕ_1 and ϕ_2 is modelled below. Moreover, an engine torque model is presented.

There are different ways to model the road. In [17] a frequency analysis shows that a road could be approximated as a first order process with a certain cut-off frequency. It is assumed in [19] that vertical road profiles could only consist of constant road grade or parabolic segments. That means that two different models of road grade would then have to be used. Their conclusion is, however, that an implementation of a model like that would be too complex and they therefore model the road grade as a slowly changing parameter, i.e, derivative equal to zero, and add a large enough process variance. That approach was also chosen in this thesis.

$$\dot{\phi}_2 = 0 + w_3 \quad (3.29)$$

where w_3 is a normally distributed white noise process, having zero mean and a variance q_3 .

The vehicle mass is constant and should only be modelled as having a zero time derivative. But, for flexibility it is also modelled with an additive white noise process w_2 , as in Equation (3.29), although its variance, q_2 , is very small.

$$\dot{\phi}_1(t) = 0 + w_2 \quad (3.30)$$

The engine torque is not measured with a sensor but estimated using a mathematical model. Since non-linearities and losses are not modelled perfectly, the engine torque was modelled with an uncertainty as in [23].

$$T_e = u_T(1 + w_1) \quad (3.31)$$

where w_1 is a normally distributed white noise process, having zero mean and a variance q_1 .

Thus, the process equation is described by

$$\dot{x} = \begin{bmatrix} \dot{v} \\ \dot{\phi}_1 \\ \dot{\phi}_2 \end{bmatrix} = \begin{bmatrix} \frac{\phi_1(u_T(1 + w_1)u_g\eta_{tf} - \alpha_1 v^2) - \alpha_2 \phi_2}{1 + \phi_1 m_r} \\ w_2 \\ w_3 \end{bmatrix} \quad (3.32)$$

For the upcoming estimator implementation it is convenient to work with difference equations instead of differential equations. The system model is therefore discretized with the Euler Method [18], which is a first-order approximation.

$$x_{k+1} \approx x_k + T_s f(x_k, u_{T,k}, w_k) \quad (3.33)$$

where T_s is the time step and subscript k denotes the discrete time instant. This yields:

$$\begin{bmatrix} v_{k+1} \\ \phi_{1,k+1} \\ \phi_{2,k+1} \end{bmatrix} = \begin{bmatrix} v_k + T_s \frac{\phi_{1,k}(u_{T,k}(1 + w_{1,k})u_g \eta_{tf} - \alpha_1 v_k^2) - \alpha_2 \phi_{2,k}}{1 + \phi_{1,k} m_r} \\ \phi_{1,k} + T_s w_{2,k} \\ \phi_{2,k} + T_s w_{3,k} \end{bmatrix} \quad (3.34)$$

3.2.2 Measurement Equation

Depending on which sensors used the measurement equation will be different. This is presented below.

Speed Measurement

$$z_k = H_1 x_k + e_k = \begin{bmatrix} 1 & 0 & 0 \end{bmatrix} x_k + e_k \quad (3.35)$$

where e_k is a normally distributed white noise process, having zero mean and a variance R_1 .

Speed and Road Grade Measurement

$$z_k = H_2 x_k + e_k = \begin{bmatrix} 1 & 0 & 0 \\ 0 & 0 & 1 \end{bmatrix} x_k + e_k \quad (3.36)$$

where e_k is a normally distributed white noise process with zero mean and a variance R_2 . The measured road grade is first translated to ϕ_2 through Equation (3.23) before being used as a measurement.

3.3 Model Validation

In order to analyse the model's correctness, acceleration predicted by the model was compared with the measured acceleration. The latter acceleration signal was created by differentiating the vehicle speed signal and then processing the signal with a low-pass filter. Performance is measured as the root mean square error, RMSE, of the acceleration.

$$RMSE = \sqrt{\frac{1}{n} \sum_{i=1}^n (\hat{a}_i - a_i)^2} \quad (3.37)$$

where a_i is the true vehicle acceleration and \hat{a}_i is the predicted acceleration for the i -th sample. Also, n is the number of samples. Vehicle parameters such as driveline efficiency, aerodynamic drag coefficient, coefficient of rolling resistance and driveline inertia were taken from data sheets or given by representatives from Volvo. Then they have been tuned manually in combination with the use of Matlab's System Identification Toolbox.

For validation of the model, true vehicle mass and road grade together with the engine torque and gear ratio were given as input to the model. True road grade is here considered to be the inclination sensor measurement. Since brake force information was not available, no validation is performed when braking.

Measurement data from the three different drive cycles described in Section 2.1 was analysed. Analysis of intervals of different acceleration magnitudes is given in Figure 3.3. According to this figure there is a trend of reaching a higher RMSE as the acceleration increases.

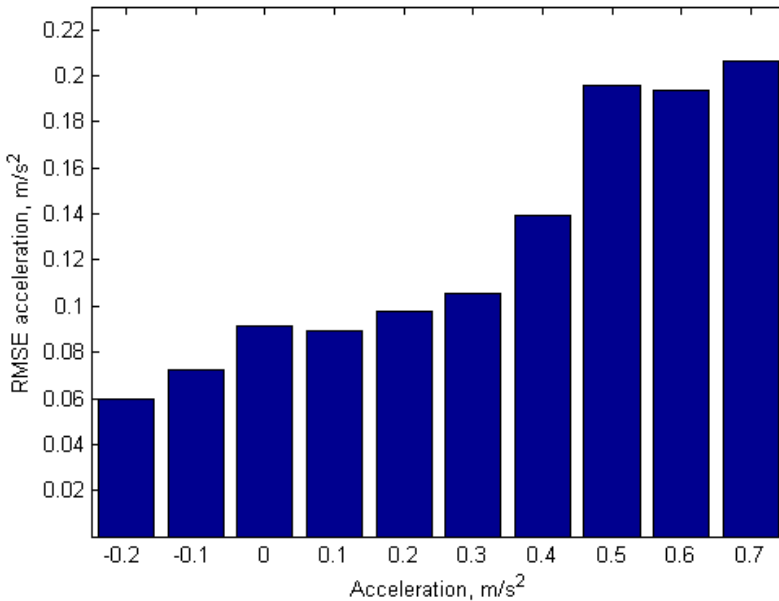


Figure 3.3. Model correctness for different acceleration intervals. The model seems to be more correct for low acceleration. Each bar corresponds to an acceleration interval, for example the bar at 0.4 m/s^2 corresponds to the interval 0.35 to 0.45 m/s^2 .

To further analyse the model, RMSE of predicted acceleration for each gear was performed. When looking at Figure 3.3 there is a larger error for lower gears. The reason why the model is worse during lower gears could be that during gear shifts there are a lot of unmodelled dynamics and non-linearities. The sudden torque changes give rise to oscillations and the driveline inertia changes as the driveline is no longer coupled. Moreover, the mathematical model that determines

the engine torque is not as accurate during transients as steady state conditions.

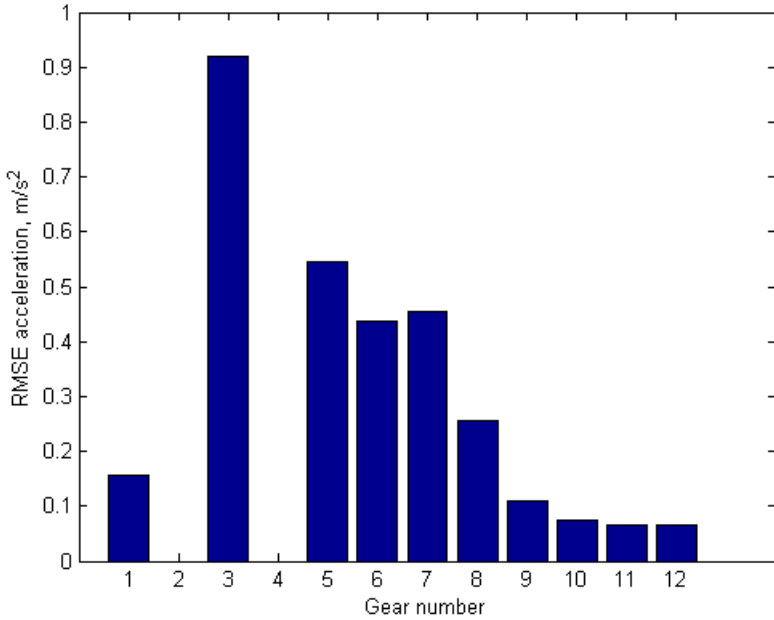


Figure 3.4. Model correctness for different gears. The model seems to be more correct for the higher gears. Observe that no data for gear number two and four was available in the analysed data sets.

The general insight of the model validation is that the model seems to be more accurate for low to moderate accelerations and the higher range of gears. Also, tests have shown that the model is not accurate during gear shifts. This knowledge is important to incorporate in the estimator.

Chapter 4

State Estimation

This chapter first presents an observability analysis of the system and then gives an explanation of the Kalman filter and the implementation of the estimator.

4.1 Observability Analysis

Observability is a necessary condition for state estimation [10]. If the system is observable, it is possible to determine the internal states by knowledge of the external outputs. It is rather simple to check observability for a linear system, but for a non-linear system it is a more complicated issue. Often it is only possible to prove observability in the neighbourhood of the actual point of operation, namely local observability. The following observability analysis follows the same methodology as in [15] and uses theory from [12]. Observability analysis is performed for the continuous model, given by the deterministic part of Equation (3.32), for the speed measurement case. This is described by:

$$\dot{x} = f(x, u) = \begin{pmatrix} f_1 \\ f_2 \\ f_3 \end{pmatrix} \quad (4.1)$$

$$z = h(x) = x_1 \quad (4.2)$$

The system is locally observable if

$$x_0 \neq x_1 \implies z(x_0) \neq z(x_1) \quad (4.3)$$

is valid in a neighbourhood of x_0 . A test for local observability at a certain operational point is that:

$$O(x, u) = \frac{\partial l(x, u)}{\partial x} \quad (4.4)$$

must have maximum rank [12]. Where,

$$l(x, u) = \begin{pmatrix} z \\ \dot{z} \\ \ddot{z} \end{pmatrix} = \begin{pmatrix} L_f^0 h \\ L_f^1 h \\ L_f^2 h \end{pmatrix} \quad (4.5)$$

and where $L_f h$ is the Lie derivative of $h(x)$ with respect to $f(x, u)$. By definition $L_f^0 h = h$ and

$$L_f^1 h = \frac{\partial h}{\partial x} \cdot f = \frac{\partial h}{\partial x} \cdot \frac{\partial x}{\partial t} = \frac{\partial h}{\partial t} = \dot{h} = \dot{z} \quad (4.6)$$

$$L_f^2 h = L_f(L_f^1 h) = L_f \left(\frac{\partial h}{\partial x} \cdot f \right) = L_f(\dot{z}) = \frac{\partial \dot{z}}{\partial x} \cdot f = \frac{\partial \dot{z}}{\partial x} \cdot \frac{\partial x}{\partial t} = \frac{\partial \dot{z}}{\partial t} = \ddot{z} \quad (4.7)$$

Thus, Equation (4.4) and (4.5), divided into the three rows of the matrix, yield

Row 1:

$$\frac{\partial}{\partial x} L_f^0 h = \frac{\partial}{\partial x} h \stackrel{Eq.(4.2)}{=} [1 \quad 0 \quad 0] \quad (4.8)$$

Row 2:

$$\frac{\partial}{\partial x} (L_f h) = \frac{\partial}{\partial x} \left(\frac{\partial h}{\partial x} \cdot \begin{pmatrix} f_1 \\ f_2 \\ f_3 \end{pmatrix} \right) \stackrel{Eq.(4.8)}{=} \frac{\partial}{\partial x} f_1 = \begin{bmatrix} \frac{\partial f_1}{\partial x_1} & \frac{\partial f_1}{\partial x_2} & \frac{\partial f_1}{\partial x_3} \end{bmatrix} \quad (4.9)$$

Row 3:

$$\frac{\partial}{\partial x} (L_f \cdot (L_f h)) \stackrel{Eq.(4.9)}{=} \frac{\partial}{\partial x} (L_f \cdot f_1) = \frac{\partial}{\partial x} \left(\frac{\partial f_1}{\partial x} \cdot \begin{pmatrix} f_1 \\ f_2 \\ f_3 \end{pmatrix} \right) = \quad (4.10)$$

$$\frac{\partial}{\partial x} \left(\frac{\partial f_1}{\partial x} \cdot f_1 \right) = \begin{bmatrix} \frac{\partial A}{\partial x_1} & \frac{\partial A}{\partial x_2} & \frac{\partial A}{\partial x_3} \end{bmatrix}, A = \frac{\partial f_1}{\partial x} \cdot f_1 \quad (4.11)$$

where it has been used that $f_2 = f_3 = 0$, which corresponds to $\dot{\phi}_1 = \dot{\phi}_2 = 0$, see Equation (3.29) and (3.30). This results in that the following matrix must have maximum rank. If using the symbols defined in Chapter 3 it writes:

$$O = \begin{bmatrix} 1 & 0 & 0 \\ \frac{\partial \dot{v}}{\partial v} & \frac{\partial \dot{v}}{\partial \phi_1} & \frac{\partial \dot{v}}{\partial \phi_2} \\ \frac{\partial A}{\partial v} & \frac{\partial A}{\partial \phi_1} & \frac{\partial A}{\partial \phi_2} \end{bmatrix}, A = \frac{\partial \dot{v}}{\partial v} \dot{v} \quad (4.12)$$

Actual calculation of the partial derivatives has here been left out. For a square matrix, it applies that the matrix has maximum rank if and only if the determinant is not equal to zero. Thus, the determinant of (4.12) gives that the following must hold for maximum rank of $O(x, u)$:

$$\frac{-2v\alpha_1\alpha_2\dot{v}}{(1 + \phi_1 m_r)^3} \neq 0 \quad (4.13)$$

Thus, the system is locally observable if (4.13) is valid, which means that vehicle speed and acceleration must be non-zero. This means that changing dynamics is necessary for simultaneous estimation of vehicle mass and road grade.

4.2 Kalman filter

This section explains the Kalman filter and a variant used for non-linear systems, the extended Kalman filter, EKF. For mathematical proofs and complete derivation, please refer to [3]. The Kalman filter was developed in 1960 by Rudolf E. Kalman and is named after him. It has gained popularity owing to computing improvements and being simple and robust. The extended Kalman filter is probably the most widely used estimation algorithm for non-linear systems. The Kalman filter has been used in many applications, for example autonomous navigation and target tracking. It estimates the state described by

$$x_k = Ax_{k-1} + Bu_{k-1} + w_{k-1} \quad (4.14)$$

$$z_k = Hx_k + e_k \quad (4.15)$$

where w_k and e_k are process and measurement noise with covariance Q and R respectively. In the list below some important properties of the Kalman filter are given.

Kalman Filter Properties

- If the process and measurement noise, w_k and e_k , have Gaussian distribution, the Kalman filter is the optimal filter among both linear and non-linear filters. It is optimal in the sense that it minimizes the estimated error covariance.
- It is recursive, which means that all measurements does not have to be stored.
- It utilizes only the two first statistical moments of the state distribution, i.e the mean and covariance.

As concluded in Section 3.1.3, the state space model describing the vehicle motion is non-linear. A common modification of the Kalman filter for non-linear dynamical systems is the extended Kalman filter. In this project only the process equation is non-linear whereas the measurement equation is linear. Using the same notation as in Chapter 3, the state space model is written as:

$$x_k = f(x_{k-1}, u_{k-1}, w_{k-1}) \quad (4.16)$$

$$z_k = h(x_k, e_k) \quad (4.17)$$

The basic operation of the Kalman filter can be divided into two update steps. See equation (4.18) and Figure 4.1. The first step projects the state in time through the state space model. This is called time update or prediction. The estimate is

called a *a priori* estimate, \hat{x}_k^- . Then feedback is obtained from the measurement. A weighted difference between the measurement and the a priori estimate is used to correct the a priori estimate. This step is called measurement update, or correction. The estimate is called a *posteriori* estimate, \hat{x}_k . The optimal gain K , which performs the weighting, is calculated by applying the Kalman filter recursions. To start the operation of the Kalman filter, initial guesses on state and state error covariance needs to be provided by the user, see Figure 4.1.

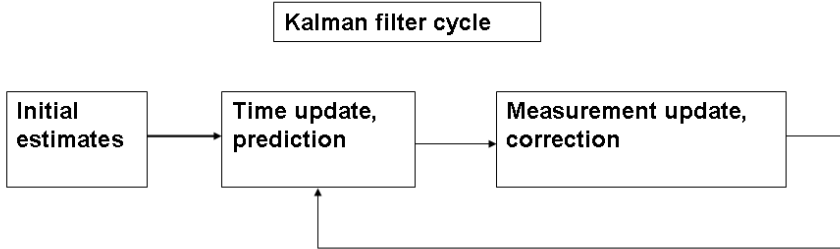


Figure 4.1. High-level description of the Kalman filter algorithm. The Time update step projects the estimated state ahead in time. The Measurement update step weighs in feedback from the measurement. The operation starts with providing an initial state guess.

$$\hat{x}_k = \hat{x}_k^- + K(z_k - H\hat{x}_k^-) \quad (4.18)$$

The EKF method first linearises the system around the current estimate, with a first order Taylor series expansion. Then the standard Kalman filter equations are applied. Optimality is now only approximated, and the linearisation error needs to be small. For more information about the Kalman filter and the EKF, please refer to [22]. Applying the EKF algorithm to (4.16) and (4.17) yields the following time and measurement updates.

Time update equations:

$$\hat{x}_k^- = f(\hat{x}_{k-1}, u_{k-1}, 0) \quad (4.19)$$

$$P_k^- = F_k P_{k-1} F_k^T + W_k Q_{k-1} W_k^T \quad (4.20)$$

Measurement update equations:

$$K_k = P_k^- H_k^T (H_k P_k^- H_k^T + R_k)^{-1} \quad (4.21)$$

$$\hat{x}_k = \hat{x}_k^- + K_k(z_k - h(\hat{x}_k^-, 0)) \quad (4.22)$$

$$P_k = (I - K_k H_k) P_k^- \quad (4.23)$$

where I is an identity matrix and F and W are Jacobian matrices defined by:

$$F = \begin{bmatrix} \frac{\partial f_1}{\partial x_1} & \cdots & \frac{\partial f_1}{\partial x_n} \\ \vdots & \ddots & \vdots \\ \frac{\partial f_m}{\partial x_1} & \cdots & \frac{\partial f_m}{\partial x_n} \end{bmatrix}, x = \hat{x}_k^-, u = u_k \quad (4.24)$$

$$W = \begin{bmatrix} \frac{\partial f_1}{\partial w_1} & \cdots & \frac{\partial f_1}{\partial w_n} \\ \vdots & \ddots & \vdots \\ \frac{\partial f_m}{\partial w_1} & \cdots & \frac{\partial f_m}{\partial w_n} \end{bmatrix}, x = \hat{x}_k^-, u = u_k \quad (4.25)$$

which applied on (3.34) yields:

$$F = \begin{bmatrix} 1 - 2T_s \frac{\alpha_1 \phi_1 v_k}{1 + \phi_1 m_r} & T_s \frac{u_T u_g \eta_{tf} + \alpha_1 v^2 + \alpha_2 \phi_2 m_r}{(1 + \phi_1 m_r)^2} & -T_s \frac{\alpha_2}{1 + \phi_1 m_r} \\ 0 & 1 & 0 \\ 0 & 0 & 1 \end{bmatrix}, x = \hat{x}_k^-, u = u_k \quad (4.26)$$

$$W = \begin{bmatrix} T_s \frac{\eta_{tf} \phi_1 u_T u_g}{1 + \phi_1 m_r} & 0 & 0 \\ 0 & T_s & 0 \\ 0 & 0 & T_s \end{bmatrix}, x = \hat{x}_k^-, u = u_k \quad (4.27)$$

Explanation of the covariance matrices WQW^T and R

For simpler notation, let $WQW^T = \bar{Q}$. The \bar{Q} and R matrices are the design variables of the Kalman filter and up to the user to set and tune. They determine how much the process and measurement equations are trusted. It is not the actual value of the elements in the matrices that are important but the relation between \bar{Q} and R . What happens when \bar{Q} and R moves to extreme values is interesting to analyse. If R moves towards zero it means that the measurement is trusted more and more. The filter will respond with a large gain. If R moves towards infinity it means that measurements are worthless and the process should be trusted.

The measurement noise is available by analysing the vehicle speed and road inclination signal. The process noise is however a tougher task to determine. Intuition was used as a foundation and manual tuning afterwards. There exist systematic methods as well, e.g the generalized autocovariance least squares tuning method [2].

For the vehicle model, Q was set to a 3×3 diagonal matrix, whereas W is defined in Equation (4.27). R is a scalar when only measuring speed and a 2×2 diagonal matrix when also measuring road inclination. The first element in R represents the variance of the speed signal and the second element represents the variance of the inclination signal.

4.3 Estimator Implementation

This section gives a high-level picture of how the developed estimator prototype was implemented in Matlab. Figure 4.2 represents an information flow. Moreover, the mass selection algorithm is presented. The block *on/off logics* consists of thresholds of the signals. When all thresholds are exceeded, the model is considered to be sufficiently accurate and system excitation sufficiently high. The criteria are given in the list below.

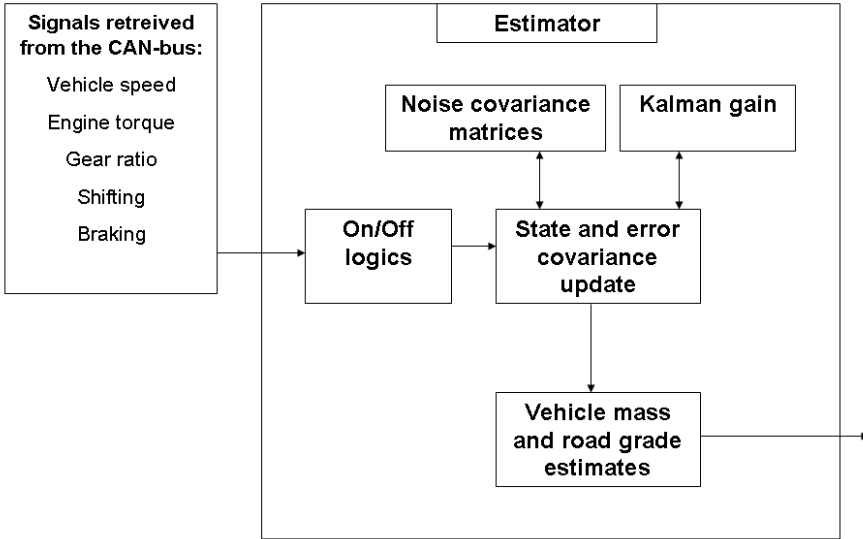


Figure 4.2. The design of the estimator on a high level.

Conditions for Estimation, On/Off Logics

- No estimation during gear shifting.
- No estimation during braking.
- Vehicle speed higher than 35 km/h.
- Engine torque higher than 200 Nm.
- Mass estimation is freed for a while if engine torque derivative is higher than 2000 Nm/s.
- Mass estimation is freed for a while if the estimator has been off for a longer period.

The first four criteria are taken as a consequence from the insights gained when validating the model, see Section 3.3. The last two criteria were found after analysis of the estimation results. When performing estimations, these factors were discovered as the cause to sudden jumps in the mass estimate. The reason why high torque derivative gives inaccurate mass estimates could be that the torque signal is not completely accurate during transients. Moreover, when the estimator has been off for a longer period, the grade estimate is far from the true value. This in combination with a low system excitation might lead to that the mass compensates for the erroneous grade estimate. Waiting a while before starting mass estimation until the grade estimate is more in line with the true grade is therefore preferable. After a reliable mass estimate, see Section 4.3, has been obtained, the estimator locks the mass to that value and starts to only estimate grade. At the same time the engine torque threshold is lowered to 0 Nm.

Mass Selection Method

The mass is chosen by applying a sliding window of the past 500 mass samples, i.e, 10 seconds. If the standard deviation of the mass samples within that window is below a certain limit the mean of the mass samples in the window is chosen as a converged mass estimate. As the window continues more and more converged mass estimates are created. After at least 15 converged mass estimates and almost five minutes, the final mass estimate is chosen as a mean of the converged mass estimates.

Chapter 5

Results

This chapter summarizes the performance of the developed estimator. The chapter is divided into three parts. The first part analyses simulated data, the second analyses real data and the third part is a sensitivity analysis. The second part, Section 5.2, is divided into one section where simultaneous estimation of vehicle mass and road grade is performed and one section where only vehicle mass is estimated. In the last mentioned case, the inclination sensor signal is used as an extra measurement. The performance is for the road grade estimate measured by the root mean square error, RMSE, see Equation (3.37) with road grade instead of acceleration. For the vehicle mass estimate, performance is measured by the relative error.

5.1 Testing with Simulated Data

The estimator is first tested on a specific case where the road grade changes as steps. Then it is tested on a realistic road. The use of the simulated data is to both validate that the estimation algorithm is correct, and to add flexibility so that different kinds of roads and driving scenarios could be tested.

5.1.1 Mass and Grade Estimation

In Figure 5.1 the basic behaviour of the estimator is shown when the grade changes as steps. The mass converges after 20 seconds to a value 1.8 % from the true mass. The RMSE of the grade is 0.21° if counting from the time of convergence of the mass estimate. Initially, before the estimates have settled, a small overshoot of the grade is visible. Moreover as the grade changes the mass gets closer and closer to the true value, which indicates that changing dynamics improves estimation, which was shown in Section 4.1. In Figure 5.2, the performance of the estimator on a realistic road can be seen. The mass error was calculated to 0.5 % and the RMSE of the grade estimate 0.02° . Both the mass and grade are initially erroneous for a while until they almost find the true values.

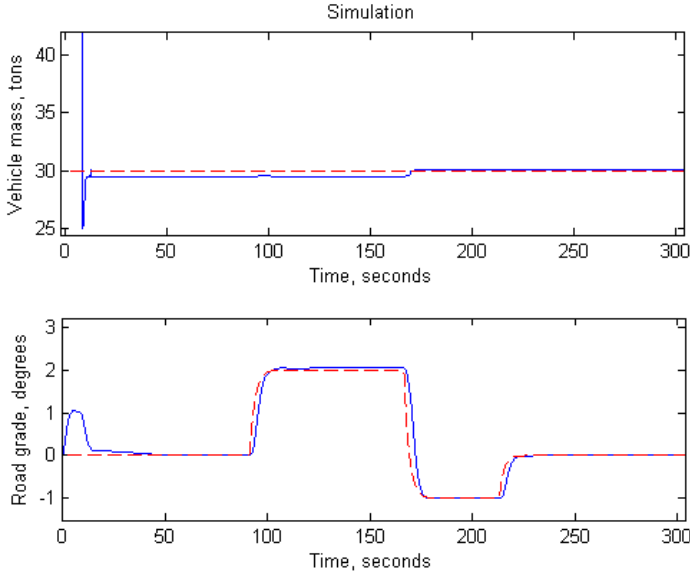


Figure 5.1. Step changes of road grade, simulated data. Dashed line represents the true values while solid line represents estimates.

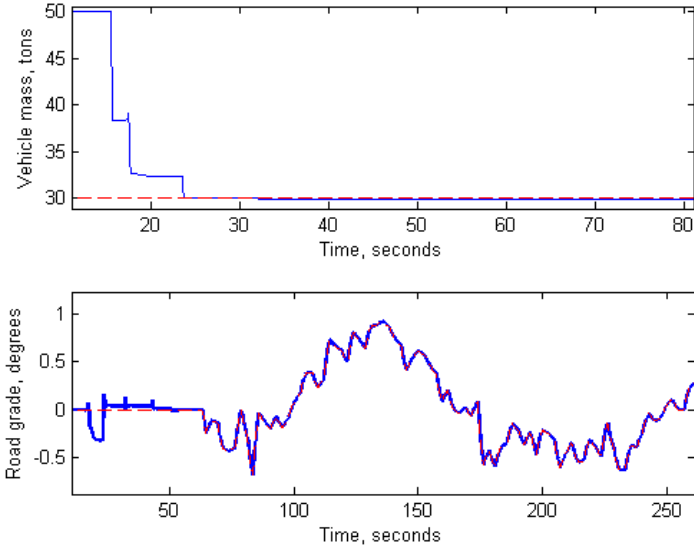


Figure 5.2. Realistic road profile, simulated data. Dashed line represents the true values while solid line represents estimates.

5.2 Testing with Real Measurement Data

In this section, the estimator is tested on real data. Section 5.2.1 evaluates the simultaneous vehicle mass and road grade estimator. Section 5.2.2 analyses the mass only estimator. The estimators tested in these two sections were tuned independently from each other. However, for each estimator the tuning parameters are kept the same throughout the testing on the three different data sets.

5.2.1 Mass and Grade Estimation

In Figure 5.3 performance on the data from the third test run is shown. The results for all three test runs are given in Table 5.1. Notice that the estimator is turned off for approximately 25 seconds due to a too low engine torque.

The time to a reliable mass estimate is around five minutes in all tests. This might seem high when noticing that the mass estimate is almost correct after 50 seconds in Figure 5.3. This longer time is however a consequence of the mass selection method, described in Section 4.3, which requires a certain number of converged mass estimates. Demanding many converged mass estimates increases the accuracy of the estimation when taking all the three test runs into consideration.

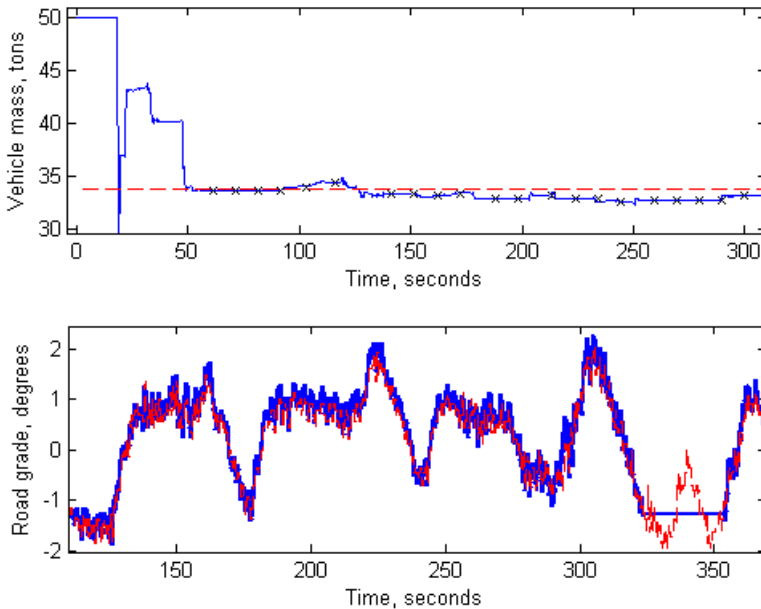


Figure 5.3. Real data, simultaneous mass and grade estimation. Dashed line represents the true values while solid line represents estimates. The crosses in the figure represent converged mass estimates.

Table 5.1. Test results when measuring vehicle speed. The 3rd column presents the RMSE for the road grade only during the time the estimator is on and all criteria defined in Section 4.3 are met.

Test run	Mass error	RMSE of grade	RMSE of grade, only when criteria are met
1	3.9 %	0.4°	0.3°
2	3.2 %	0.5°	0.3°
3	1.6 %	0.4°	0.3°

5.2.2 Mass Estimation

When having the inclination sensor as an extra measurement, the mass estimation becomes more robust and accurate, see Figure 5.4 and Table 5.2. Vehicle mass error is now around 1 % for the three different test runs.

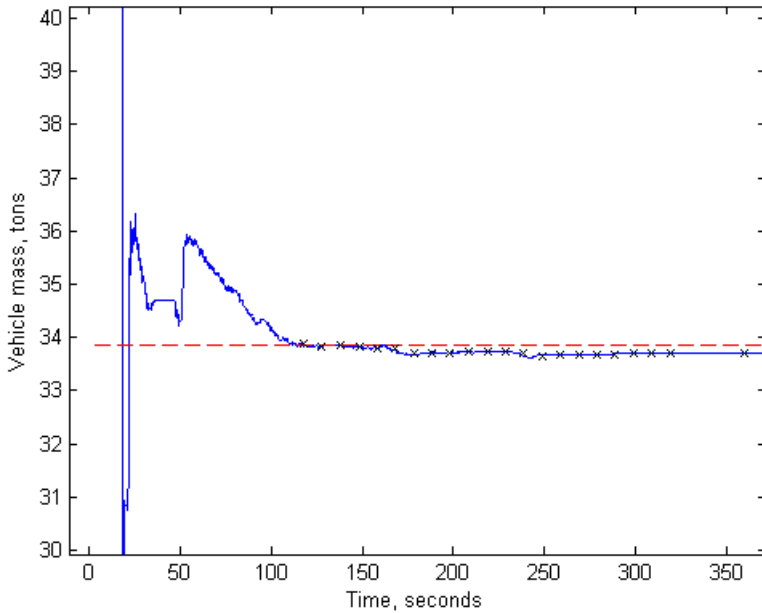


Figure 5.4. Mass estimation, real data, inclination sensor is used as additional measurement. Dashed line represents the true values while solid line represents estimates. The crosses in the figure represent converged mass estimates.

Table 5.2. Test results when measuring vehicle speed and road grade.

Test run	Mass error
1	0.52 %
2	1.2 %
3	0.49 %

5.3 Sensitivity Analysis

The sensitivity analysis was performed for the mass and grade estimation case. The analysis was done by varying one parameter at the time and see how this affects the vehicle mass and road grade error. First, three parameters from the vehicle model are analysed; aerodynamic drag coefficient, c_d , coefficient of rolling resistance, f_r , and inertia of wheels and axle shafts, J_w . Then, the measurement noise covariance R is analysed. This analysis does not compare with the true values, but with the estimates given by the estimator for one of the test runs. Hence, in the figures below the estimates reach zero for the parameter value that were chosen in the estimator implementation. This is to more clearly see how the estimates change when the parameters are varied. Figures 5.5-5.8 show that they influence the vehicle mass and road grade estimates slightly. However, estimates are not dramatically changed. For each parameter, a short analysis is given in the caption in the corresponding figure.

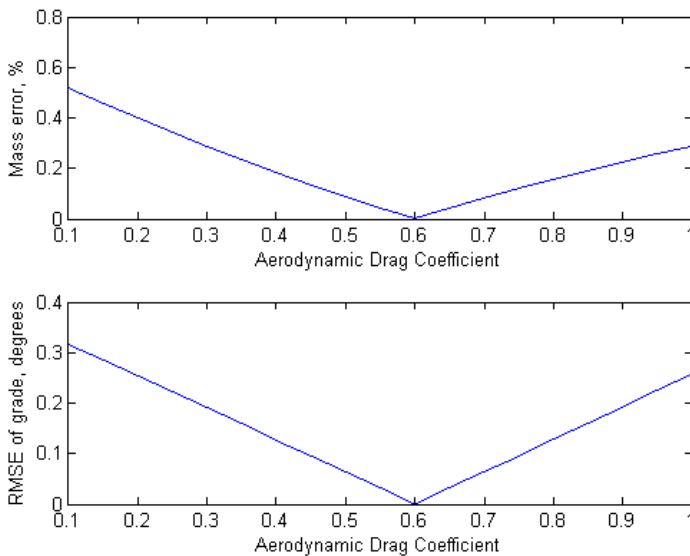


Figure 5.5. Sensitivity for aerodynamic drag coefficient, c_d . The road grade is sensitive for this coefficient while vehicle mass is rather insensitive.

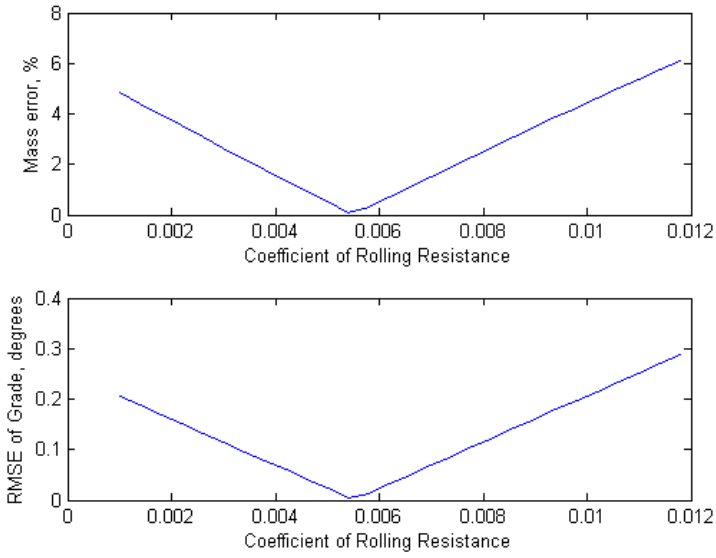


Figure 5.6. Sensitivity for the coefficient of rolling resistance, f_r . Both vehicle mass and road grade are sensitive for this coefficient.

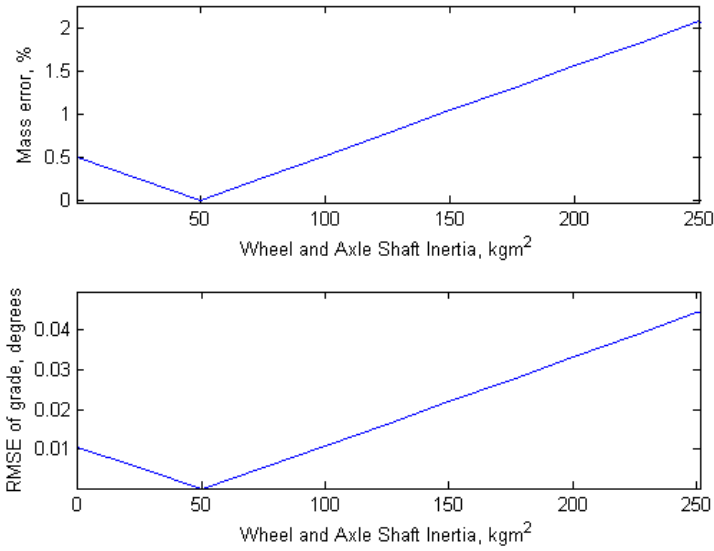


Figure 5.7. Sensitivity for the wheel and axle shaft inertia, J_w . Road grade estimate is insensitive for this coefficient while the vehicle mass is rather sensitive.

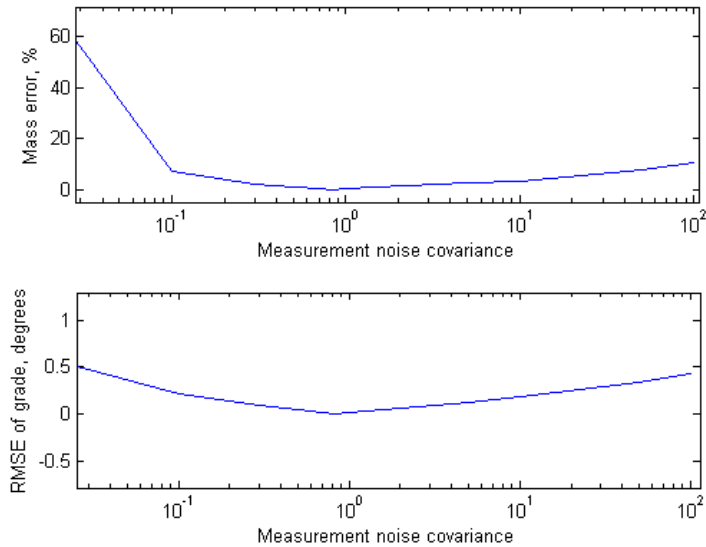


Figure 5.8. Sensitivity for measurement noise covariance, R . When the value reaches closer towards zero the mass estimate gets very erroneous. Besides, mass and grade estimates are not very sensitive for this parameter.

Chapter 6

Conclusions and Future Work

The purpose of this thesis is to perform vehicle mass and road grade estimation. One estimator for simultaneous estimation of vehicle mass and road grade was developed. Also a mass estimator, additionally using a road inclination sensor was developed. Both estimators use an extended Kalman filter (EKF). The estimators were evaluated on both simulated and real measurement data, collected with a truck on road. An observability analysis was performed to provide a mathematical ground for the estimations. To analyse the robustness, a sensitivity analysis was performed.

6.1 Conclusions

It has been found that the estimators are giving acceptable results, both when testing on simulated and on real measurement data. For the case of using real measurement data and simultaneously estimating vehicle mass and road grade, the mass estimate error is often within 5 % and the grade estimate root mean square error is often within 0.6° . The mass estimator, using the inclination sensor, is more accurate, robust and quicker than the mass and grade estimator. Mass error is often within 2 % for this method. The observability analysis showed that the system is locally observable if the vehicle acceleration is non-zero. The sensitivity analysis showed that the estimator is somewhat sensitive to changes in vehicle and the tuning parameters of the Kalman filter. But for small parameter variations the estimator is fairly robust.

6.2 Future Work

Some possibilities for future work are listed below:

- More analysis of the engine torque signal and investigate when it is reliable and not.
- When the inclination sensor is used, extend to estimate an additional parameter to vehicle mass.
- Improve the vehicle model, and more accurately model the forces in the force balance equation.
- Use altitude information, for example through a GPS receiver. During this project, some work was done in simulation with altitude as an extra measurement with quite promising results.

Bibliography

- [1] *Automotive Handbook*. Robert Bosch GmbH, 3 edition, 1993.
- [2] Bernt M. Akesson, John Jorgensen Bagterp, Niels Kjolstad Poulsen, and Sten Bay Jorgensen. A tool for kalman filter tuning. In *17th European Symposium on Computer Aided Process Engineering - ESCAPE17*, 2007.
- [3] Brian D.O. Anderson and John B. Moore. *Optimal Filtering*. Prentice-Hall, 1979.
- [4] Hong S. Bae, Johan Ryu, and Gerdes Christian J. Road grade and vehicle parameter estimation for longitudinal control using gps. In *Proc.of IEEE Conf. on Intelligent Transportation Systems*, 2001.
- [5] Anders Eriksson. Implementation and evaluation of a mass estimation algorithm. Master's thesis, KTH, 2009.
- [6] Hosam K. Fathy, Dongsoo Kang, and Jeffrey L. Stein. Online vehicle mass estimation using recursive least squares and supervisory data extraction. In *American Control Conference*, 2008.
- [7] Lei Feng. Prestudy: Vehicle mass and road grade estimation, er-59266. Technical report, Volvo Technology, 2010.
- [8] Johan Georgii and Gabriel Ringius. Mass determination - online estimation for heavy duty vehicles. Master's thesis, Chalmers University of Technology, 2009.
- [9] Thomas D. Gillespie. *Fundamentals of Vehicle Dynamics*. Society of Automotive Engineers, Inc., 2 edition, 1992.
- [10] Fredrik Gustafsson, Lennart Ljung, and Mille Millnert. *Signalbehandling*. Studentlitteratur, 2008.
- [11] K. Hayakawa, R. Hibino, M. Osawa, S. Sonoda, T. Murahashi, N. Yamada, and H. Kato. On-board estimation of vehicle weight by optimizing signal processing. In *2006 SAE World Congress Detroit, Michigan*. 2006.
- [12] J.K. Hedrick and A. Girard. *Controllability and Observability of Nonlinear Systems*. 2005. Class Notes.

-
- [13] Jonas Hellgren. Kalman filter based road slope estimation from speed and altitude measurements. Technical report, Volvo Technology, 2010.
 - [14] Ken Johansson. Road slope estimation with standard truck sensors. Master's thesis, KTH, 2005.
 - [15] Uwe Kiencke and Lars Nielsen. *Automotive Control Systems, For Engine, Driveline and Vehicle*. Springer, 2 edition, 2005.
 - [16] Marcus Larsson and Anders Schantz. Route recognition from recorded inclination data enabling use of preview-based fuel-saving functions. Master's thesis, Chalmers University of Technology, 2008.
 - [17] Peter Lingman and Bengt Schmidtbauer. Road slope and vehicle mass estimation using kalman filtering. In *Proceedings of the 17th IAVSD symposium*, 2001.
 - [18] Lennart Ljung and Torkel Glad. *Modellbygge och Simulering*. Studentlitteratur, 2 edition, 2004.
 - [19] Per Sahlholm. *Iterative Road Grade Estimation for Heavy Duty Vehicle Control*. KTH, 2008. Licentiate Thesis.
 - [20] Paul Schmitt. Test report - load and grade estimator project. Technical report, Volvo Powertrain NA, 2010.
 - [21] Ardalan Vahidi, Anna Stefanoupolou, and Huei Peng. Experiments for on-line estimation of heavy vehicle's mass and time-varying road grade. In *Proceedings of IMECE, Washington DC*, 2003.
 - [22] Greg Welch and Gary Bishop. *An Introduction to the Kalman Filter*. University of North Carolina at Chapel Hill, 2006.
 - [23] Vincent Winstead and Ilya V. Kolmanovsky. Estimation of road grade and vehicle mass via model predictive control. In *Proceedings of the 2005 IEEE Conference on Control Applications*, 2005.